European Radiology (2019) 29:468–475
https://doi.org/10.1007/s00330-018-5590-0

ONCOLOGY

Clustering approach to identify intratumour heterogeneity combining FDG PET and diffusion-weighted MRI in lung adenocarcinoma

Jonghoon Kim[1] · Seong-Yoon Ryu[2] · Seung-Hak Lee[1] · Ho Yun Lee[2] · Hyunjin Park[3,4]

Received: 26 March 2018 / Revised: 13 May 2018 / Accepted: 4 June 2018 / Published online: 19 June 2018
© European Society of Radiology 2018

Abstract

Objectives Malignant tumours consist of biologically heterogeneous components; identifying and stratifying those various subregions is an important research topic. We aimed to show the effectiveness of an intratumour partitioning method using clustering to identify highly aggressive tumour subregions, determining prognosis based on pre-treatment PET and DWI in stage IV lung adenocarcinoma.

Methods Eighteen patients who underwent both baseline PET and DWI were recruited. Pre-treatment imaging of SUV and ADC values were used to form intensity vectors within manually specified ROIs. We applied k-means clustering to intensity vectors to yield distinct subregions, then chose the subregion that best matched the criteria for high SUV and low ADC to identify tumour subregions with high aggressiveness. We stratified patients into high- and low-risk groups based on subregion volume with high aggressiveness and conducted survival analyses. This approach is referred to as the partitioning approach. For comparison, we computed tumour subregions with high aggressiveness without clustering and repeated the described procedure; this is referred to as the voxel-wise approach.

Results The partitioning approach led to high-risk (median SUVmax = 14.25 and median ADC = $1.26\text{x}10^{-3}$ mm^2/s) and low-risk (median SUVmax = 14.64 and median ADC = $1.09\text{x}10^{-3}$ mm^2/s) subgroups. Our partitioning approach identified significant differences in survival between high- and low-risk subgroups (hazard ratio, 4.062, 95% confidence interval, 1.21 – 13.58, *p*-value: 0.035). The voxel-wise approach did not identify significant differences in survival between high- and low-risk subgroups (*p*-value: 0.325).

Conclusion Our partitioning approach identified intratumour subregions that were predictors of survival.

Key Points

- *Multimodal imaging of PET and DWI is useful for assessing intratumour heterogeneity.*
- *Data-driven clustering identified subregions which might be highly aggressive for lung adenocarcinoma.*
- *The data-driven partitioning results might be predictors of survival.*

Keywords Clustering analysis · Survival analysis · Adenocarcinoma of lung · Intratumour heterogeneity · Multimodal imaging

✉ Ho Yun Lee
hoyunlee96@gmail.com

✉ Hyunjin Park
hyunjinp@skku.edu

[1] Department of Electronic Electrical and Computer Engineering, Sungkyunkwan University, Suwon, Korea

[2] Department of Radiology and Center for Imaging Science, Samsung Medical Center, Sungkyunkwan University School of Medicine, 50 Ilwon-Dong, Kangnam-Ku, Seoul 06315, Korea

[3] School of Electronic and Electrical Engineering, Sungkyunkwan University, Suwon 16419, Korea

[4] Center for Neuroscience Imaging Research, Institute for Basic Science, Suwon, Korea

Abbreviations

DCR	Disease control rate
HR	Hazard ratio
ORR	Overall response rate
OS	Overall survival
PFS	Progression free survival

Introduction

Malignant tumours are biologically complex and manifest substantial spatial variation in vascularity, metabolism, histologic differentiation, biochemistry, and macroscopic

structure [1], which are predicated by genomic heterogeneity [2]. This intratumour heterogeneity of genomic origin might indicate a poor prognosis [3]. Some studies reported subpopulations of cells that show resistance to therapy [4, 5]. Nevertheless, modern cancer treatment is typically based on accurate tissue diagnosis of samples obtained from needle biopsy or surgical excision. Lung adenocarcinoma, especially, is highly heterogeneous and usually has variable combinations of two or more histologic subtype patterns [6]. Management of approximately 80% of advanced or inoperable cases usually relies on a limited sample of cancer tissue that cannot represent intratumour heterogeneity. Therefore, recognition of intratumour heterogeneity to inform treatment decisions requires sophisticated imaging analysis methods that could fully capture the potential heterogeneity of the whole tumour [7].

Imaging-based quantitative stratification of lung adenocarcinoma plays an essential role in diagnosis, staging, therapeutic planning, and response evaluation [8–10]. Positron emission tomography (PET) reflects tumour metabolism [11]. Diffusion-weighted magnetic resonance imaging (DWI) captures tissue cellularity and microstructure, and the apparent diffusion coefficient (ADC), a measure derived from DWI, is widely used for tumour differentiation [12]. A multimodal study is capable of integrating complementary information to better assess tumour hallmarks compared with a single-mode study [13, 14]. Lee et al explored successful prognostic stratification of lung adenocarcinoma using DWI and PET [15]. We adopted these two functional imaging measures, ^{18}F-fluorodeoxyglucose (FDG) uptake of PET and ADC in DWI, to differentiate heterogeneous intratumour subregions according to two important tumour properties of glucose metabolism and cell differentiation and apoptosis.

Intratumour heterogeneity is often difficult to assess with the naked eye, and recent developments in machine learning have contributed significantly toward enhanced quantification of such heterogeneity [16–18]. Partitioning a whole tumour refers to dividing the whole volume into smaller subregions, which often allows better quantification of intratumour heterogeneity. We applied a data-driven clustering algorithm to partition the whole tumour volume into subregions of different degrees of tumour aggressiveness. We aimed to show the effectiveness of an intratumour partitioning framework based on the integrated analysis of PET and DWI in patients with lung adenocarcinoma. We hypothesised that subregions that appear to have lower ADC and higher FDG uptake reflect areas of highly aggressive tumour and ultimately determine prognosis. In addition, we compared the performance of a partitioning-based approach and a voxel-based approach in terms of recognition of intratumour heterogeneity.

Materials and methods

Patient population

This prospective study was approved by our Institutional Review Board and written informed consent was obtained from all patients (IRB # 2011-05-087-001). We recruited a total of 31 patients with stage IV lung adenocarcinoma. All patients received both baseline PET/CT and DWI imaging before platinum-based chemotherapy as a first-line therapy. Patients were excluded based on the following criteria: (1) lack of informed consent (n=5), (2) primary tumour less than 2 cm (n=2) considering the potential measurement error of the ADC map derived from the limited spatial resolution, (3) receiving concurrent chemoradiotherapy (CCRT) (n=2), (4) missing baseline PET or CT images (n=3), and (5) misalignment between DWI and PET image (n=1). We analysed 18 patients according to the exclusion criteria in Figure 1.

Image acquisition

DWI images were obtained using a 1.5 Tesla (T) scanner (Magnetom Avanto, Siemens, Erlangen, Germany) with the following parameters: single shot spin echo EPI sequence with spectral selection attenuated inversion recovery; repetition time/echo time, 11700/73 ms; EPI factor, 142; number of excitations, 4; field of view (FOV), 400 × 325 mm; imaging matrix, 192 × 142; and slice thickness, 5 mm. PET images were obtained from the PET/CT protocol. Patients were injected with 370 MBq (10 mCi) of FDG and then scanned on a GE Discovery PET/CT scanner (Discovery LS; GE Healthcare) that included a PET scanner (Advanced NXi; GE Medical Systems) for 60 minutes. Contrast agent was delivered by intravenous bolus injection at a flow rate of approximately 0.1 mmol/kg (Gadoterate meglumine, Dotarem, Guerbet LLC, New Jersey, USA). PET data were acquired in a 2-dimensional mode with 3 to 5 minutes of acquisition time per bed position. The PET images were then reconstructed with an ordered set expectation maximisation algorithm. The spatial resolution of the PET image was 3.91 × 3.91 × 3.27 mm^3.

Image processing and partitioning

Raw PET values were converted to SUV. The ADC map was computed in a voxel-wise fashion using the Stejskal-Tanner formula with b = 0, 100, and 700 s/mm^2. Primary tumour ROIs were drawn manually by one expert (HYL) with 15 years of experience. Figure 2 shows an overview of the imaging processing procedures, which consisted of the following steps. First, intra-patient registration was performed to spatially align DWI and PET images for each patient using an affine

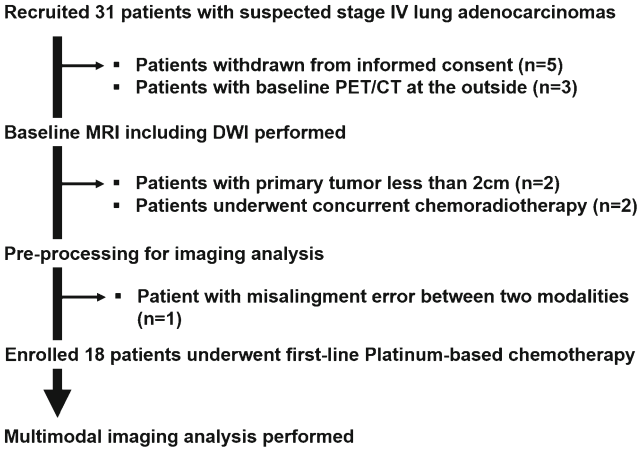

Fig. 1 Study enrolment criteria

transformation. This process enabled us to obtain the intensities on the same coordinate in multimodal analysis. We applied k-means clustering (k = 4) to registered DWI and PET data to yield four distinct subregions. We initialised the k-means algorithm based on Arthur et al and repeated procedure 10 times [19]. We then selected the clustering result that was most stable for the 10 clustering results based on Rand index [20]. We decided to use k of four so that the ROI into four subregions based on the possible permutations of high/low (i.e., two choices) SUV and high/low (i.e., two choices) ADC. We assumed there were four distinct potential functional subregions identifiable by PET and DWI as follows: (1) necrotic subregion showing high ADC and low SUV, (2) subregion with low tumour aggressiveness showing low ADC and low SUV, (3) subregion with high tumour aggressiveness showing low ADC and high SUV, and (4) subregion with moderate tumour aggressiveness and treatment resistance showing high ADC and high SUV. Categories (1) and (3) were previously reported [21, 22], but categories (2) and (4) were potential assignments. In our study, a subregion with high SUV and low ADC was defined as region of high tumour aggressiveness. Threshold values to

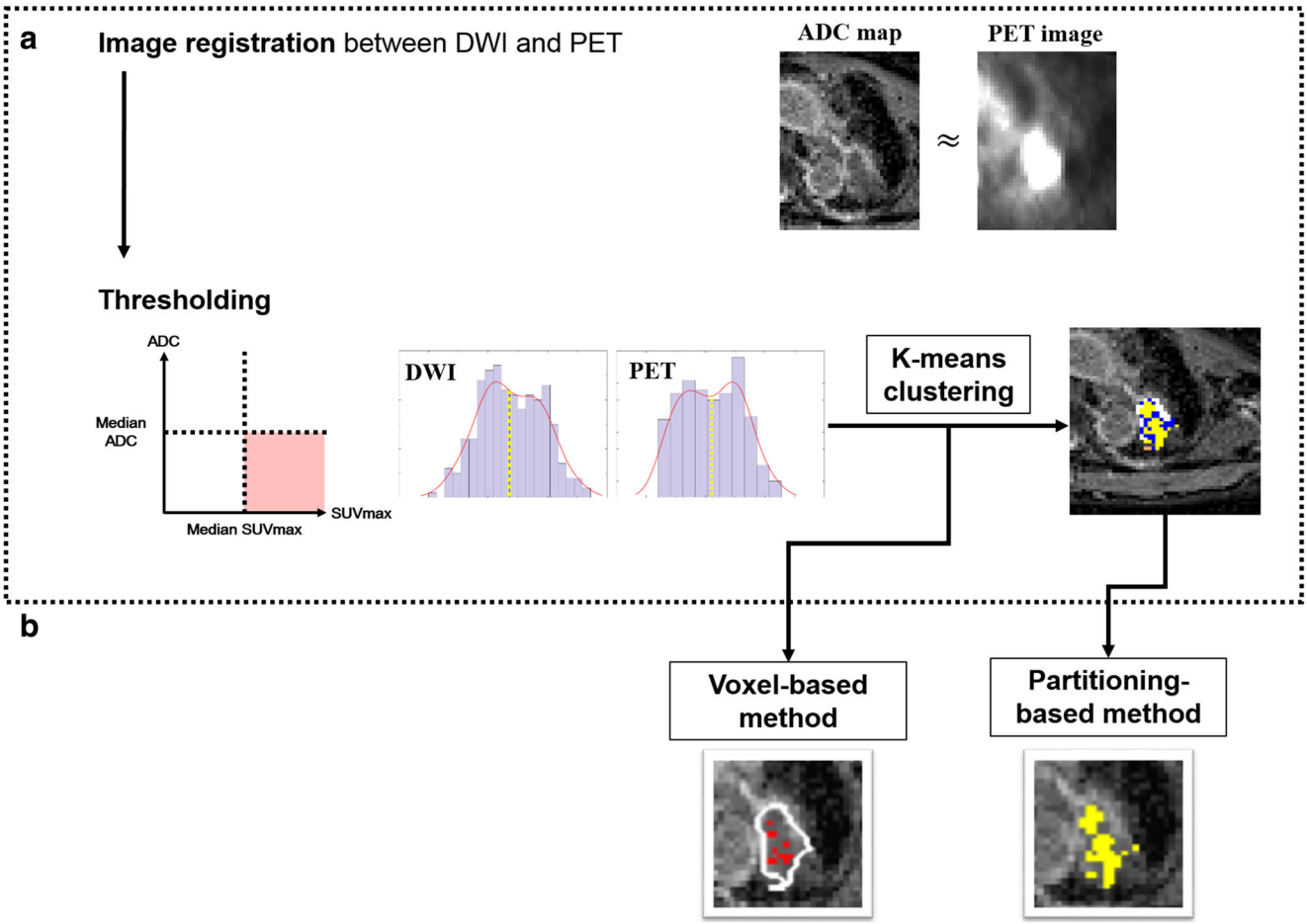

Fig. 2 Overall processing steps. Overall processing included two parts. Part (**a**) was image registration, thresholding, and k-means clustering. Raw DWI and PET images were co-registered and tumour regions with high aggressiveness within the ROI for each modality were determined using the threshold of the median value. K-means clustering (k=4) was performed to define computed subregions that would be used later for the portioning-based approach. Part (**b**) computed the hot spot within the tumour using two approaches: (1) a voxel-based method (left, using the threshold rule only) and (2) a partitioning-based method (right, using both the threshold rule and clustering). The imaging PET/ADC maps shown are representative figures

dichotomise high and low values in each modality were the median of each intensity distribution. One subregion (out of four) with the most high SUV and low ADC voxels was chosen as the subregion of high tumour aggressiveness. This method for computing tumour regions with high aggressiveness is referred to as the partitioning approach.

For comparison, we computed tumour regions with high aggressiveness using the same criterion applied to all registered DWI and PET voxels, rather than the clustered subregions. This method of computing tumour regions with high aggressiveness is referred to as the voxel-wise approach.

For the partitioning-based approach, we applied k-means clustering and then applied thresholding rules to identify the tumour subregion with high aggressiveness. For the voxel-wise approach, we did not apply clustering and just applied thresholding rules to identify the tumour subregion with high aggressiveness.

Statistical analysis

We computed tumour regions with high aggressiveness for each patient using the procedures described in the previous section and sorted them with respect to the volume of the tumour regions with high aggressiveness. Patients were assigned to high- or low-risk subgroups based on the median value for the volume of the tumour region with high aggressiveness. For comparison, we stratified patients into high- or low-risk subgroups based on whole tumour volume (rather than the volume of the highly aggressive subregions). We performed the cross-validated survival curves and permutation tests [23]. In detail, a leave-one-out cross validation (LOOCV) was applied to survival analysis. For the training portion, we computed the threshold (i.e., median) to dichotomise high-risk and low-risk subgroups from 17 samples. For the test portion, the pre-determined threshold was applied to the left-out sample, and it was assigned to either high-risk or low-risk. The procedure was repeated 18 times, each time leaving a different sample out. This led to the cross-validated survival curve which was assessed with Kaplan-Meier analysis and log-rank statistics. To evaluate the statistical significance of the log-rank statistic, we performed a permutation test of the cross-validated survival curves. A null distribution of log-rank statistics was computed by random assignment of survival information 1,000 times. Statistical significance (corrected p-value) was determined if the log-rank statistic belonged outside of the 95% of the null distribution. Furthermore, we performed an outlier analysis using z-scores for the three approaches. Level of significance was set at a p-value of 0.05. Statistical analyses were performed using MATLAB (The Mathworks Inc., Natick, MA, USA).

Results

Patient characteristics

We recruited a total of 31 patients with stage IV lung adenocarcinoma who received baseline PET and DWI imaging before therapy. We analysed 18 patients according to the exclusion criteria. Of 18 patients, 11 were male. Patient ages ranged from 26-70 and the mean ± standard deviation (SD) was 52.2 ± 13.6 years. Disease control rate (DCR) was 85.7% and overall response rate (ORR) was 66.7%. The mean progression free survival (PFS) was 5.5 ± 4.6 months and average overall survival was 22.0 ± 20.5 months. Ten patients were smokers, whereas eight patients never smoked. For Eastern Cooperative Oncology Group (ECOG) performance status, three patients scored 0 and the remaining patients scored 1. Four patients survived, and 14 patients died.

Identification of tumour regions with high aggressiveness

In our study, a subregion with high standardised uptake value (SUV) and low ADC was defined as a region of high tumour aggressiveness. The threshold to determine the tumour regions with high aggressiveness was the median value for both PET and ADC, respectively. The tumour regions with high aggressiveness were computed by two approaches. One is the voxel-wise approach where we applied the threshold rule to all voxels and the other is the partitioning approach where we applied additional steps of data-driven clustering besides the threshold rule. Using the partitioning approach, we stratified the patients into high-risk and low-risk subgroups using the median (9.67cc) of tumour volume with high aggressiveness. The high-risk subgroup had median SUVmax of 14.25 and median ADC of $1.26\text{x}10^{-3}$ mm^2/s computed over the subregions with high tumour aggressiveness. The low-risk subgroup had median SUVmax of 14.64 and median ADC of $1.09\text{x}10^{-3}$ mm^2/s. For comparison, we stratified the patients into high-risk and low-risk subgroups based on whole tumour volume, rather than the volume of the highly aggressive subregions. Using the voxel-wise approach, we stratified the patients into high-risk and low-risk subgroups using the median (7.45cc) of tumour volume with high aggressiveness. The high-risk subgroup had median SUVmax of 14.20 and median ADC of $1.11\text{x}10^{-3}$ mm^2/s. The low-risk subgroup had median SUVmax of 14.49 and median ADC of $0.96\text{x}10^{-3}$ mm^2/s. Figure 3 shows representative cases of tumour regions with high aggressiveness using the partitioning and voxel-wise approaches. The partitioning based approach led to tumour regions with high aggressiveness that were spatially more contiguous and more biologically plausible. We also performed

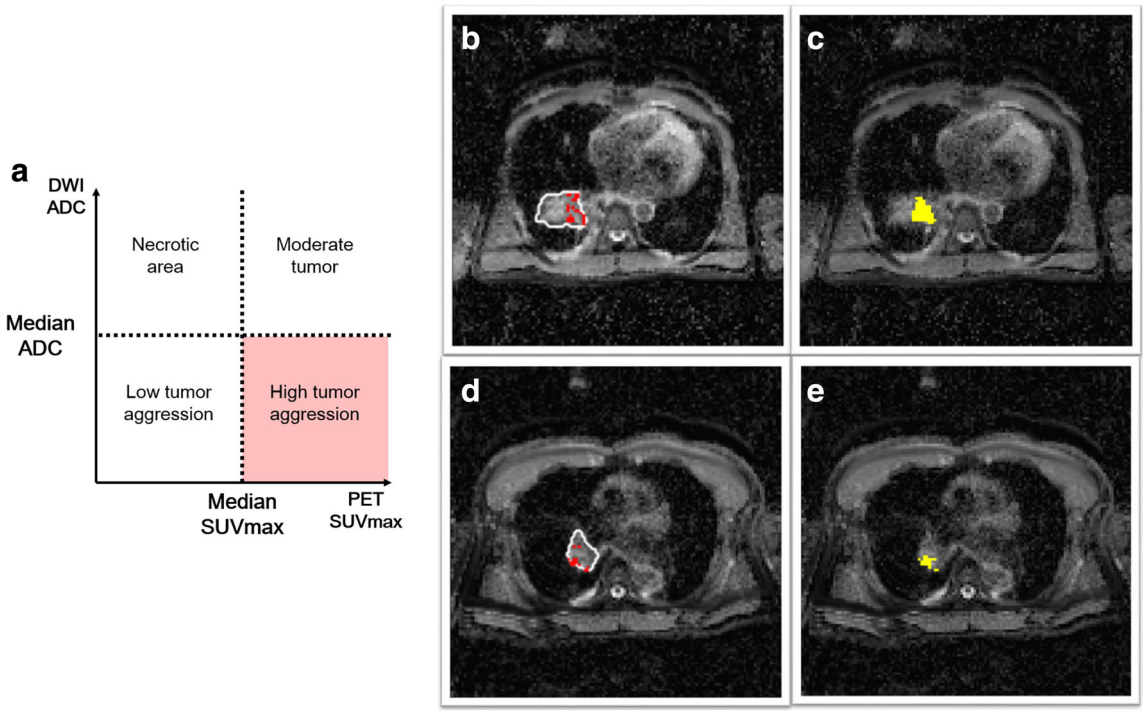

Fig. 3 Tumour regions with high aggressiveness using partitioning and voxel-wise approaches. We determined regions of high tumour aggressiveness as the colored area shown on the quartile plot (Fig. 3a). Figure 3b–e show representative cases. Figure 3b, c are images showing a relatively large tumour region with high aggressiveness from a 56-year-old male with progressive disease who survived 1.4 months. Figure 3d, e are images showing a relatively small tumour region with high aggressiveness in a 61-year-old female with the partially responsive disease who survived 71.9 months. Figure 3b, d represent tumour regions with high aggressiveness using a voxel-based method (red), where white boundaries are tumour contours of manual annotations. Figure 3c, e represent tumour regions with high aggressiveness using a partitioning-based method (yellow). Note that the representative images are 2D slices from 3D cases

an outlier analysis using z-scores for the three approaches. No outliers were identified (i.e., z-scores < 3).

Performance of survival models

Patients were assigned to high- or low-risk subgroups based on a threshold for the volume of the tumour region with high aggressiveness. The threshold was the median value of high aggressive volume for patients. For comparison, we stratified patients into high- or low-risk subgroups based on whole tumour volume, rather than the volume of the highly aggressive subregions. We performed survival analyses for high- and low-risk subgroups using Kaplan-Meier analysis. Using the partitioning approach to define tumour regions with high aggressiveness, the difference in survival between high- and low-risk subgroups was significant (hazard ratio: 4.062, 95% confidence interval: 1.21 – 13.58, p-value: 0.035). The difference in survival between high- and low-risk subgroups was not significant using the voxel-wise approach (p-value: 0.325) or conventional whole tumour volume (p-value: 0.357). The results of survival analyses are presented in Figure 4. We obtained significant results only when the partitioning approach was adopted to define tumour regions with high aggressiveness.

Discussion

In malignant tumours, populations of genetically distinct subclones can intermingle or be spatially separated, and this subclonal architecture varies dynamically throughout the disease course [24, 25]. Intratumour heterogeneity of genomic origin could be used to identify imaging biomarkers that could guide clinical decision making in cancer medicine [26]. In any case, a single biopsy is unable to represent the full tumour mutational spectrum. Genomic instability indices have been associated with poor outcomes, since different subregions harbor different levels of genomic rearrangement, therefore prognostic strategies based on single biopsy samples are likely limited by intratumour heterogeneity [27].

Non-invasive imaging-based evaluations could be an alternative to biopsies for assessing the full spectrum of intratumour heterogeneity. In this study, we proposed four distinct functional subregions identifiable by PET and DWI. We focused on the tumour regions with high aggressiveness based on high SUV and low ADC. The partitioning-based approach led to the identification of tumour regions that were significant predictors of survival. Thus, these results point to the potential added prognostic value of assessing tumour heterogeneity using the partitioning based approach.

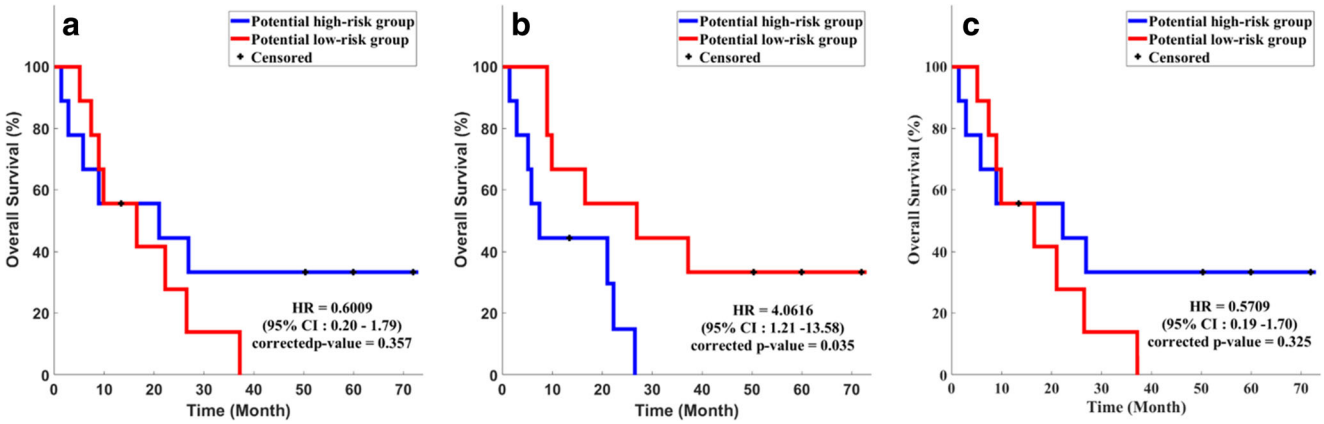

Fig. 4 Results of survival analyses. a Kaplan-Meier plot for whole tumour volume. **b** Kaplan-Meier plot for the partitioning-based approach. **c** Kaplan-Meier plot for the voxel-wise approach. Potential high-risk subgroup refers to the patients whose volume of high tumour aggressiveness is larger than the median depending on various approaches. Potential low-risk subgroup refers to the patients whose volume of high tumour aggressiveness is less than the median depending on various approaches

Others have explored the application of data-driven machine learning methods to assess intratumour heterogeneity, mainly in animal studies [28–30]. Our study is a human imaging study that proposes a robust intratumour partitioning approach to identify clinically relevant subregions with high aggressiveness. Wu et al identified high-risk subregions using FDG-PET and computed tomography (CT) and demonstrated that the tumour burden of the high-risk subregions was a prognostic factor of survival based on data-driven clustering [31]. Our study is similar to that of Wu et al, but we used a more sensitive functional modality (i.e., DWI) and assumed four distinct subregions with plausible biological interpretation.

We computed subregions with high aggressiveness within the tumour using two approaches, voxel-based and partitioning-based methods. In the voxel-based method, tumour regions with high aggressiveness were determined using the median of each modality of the tumour. Although this process could provide a collection of voxels that meet the aggressiveness criteria of both high metabolism and cellularity in PET and DWI, the result did not significantly predict patient survival (p-value: 0.325). One possible reason could be that individual voxels are influenced by intrinsic noise introduced by various parts of the acquisition process. In contrast, the partitioning-based approach clusters the voxels into four distinct clusters and each cluster has a similar intensity vector. All the voxels are mapped to one of the four clusters, and voxels in each cluster have similar intensity vectors within the given cluster. For example, a cluster with low ADC and high SUV might aggregate all voxels that are similar in intensity vector, but a voxel-wise approach might aggregate voxels who strictly satisfy low ADC and high SUV (threshold of median). Noise perturbs the signal intensities and some voxels belonging to the subregion of high aggressiveness might be erroneously mapped as the non-aggressive subregion under the voxel-wise approach. They still could be correctly mapped to the subregion with high aggressiveness under the partitioning-based approach. The partitioning approach identified tumour regions with high aggressiveness well, leading to good survival prediction (HR: 4.062, p-value: 0.035).

We reported imaging statistics for the four clusters using the partitioning approach. The first cluster with high ADC and low SUV had mean $1.49\text{x}10^{-3}$ mm^2/s (SD = $0.32\text{x}10^{-3}$ mm^2/s) in ADC and mean 8.96 (SD = 4.15) in SUVmax. The second cluster with low ADC and low SUV had mean $0.82\text{x}10^{-3}$ mm^2/s (SD = $0.26\text{x}10^{-3}$ mm^2/s) in ADC and mean 8.95 (SD = 3.97) in SUVmax. The third cluster with low ADC and high SUV had mean $1.18\text{x}10^{-3}$ mm^2/s (SD = $0.21\text{x}10^{-3}$ mm^2/s) in ADC and mean 14.05 (SD = 4.99) in SUVmax. The fourth cluster with high ADC and high SUV had mean $1.58\text{x}10^{-3}$ mm^2/s (SD = $0.33\text{x}10^{-3}$ mm^2/s) in ADC and mean 11.33 (SD = 4.46) in SUVmax. There were significant differences between the first cluster (necrotic subregion) and the third cluster (subregion with high tumour aggressiveness) using t-test (p-values 0.002 and 0.002 for ADC and SUVmax, respectively). Thus, the imaging findings of the selected subregion were consistent with existing literature [15, 21, 22].

We identified tumour subregions with high aggressiveness using the partitioning approach, which were further dichotomised into high-risk and low-risk subgroups. The high-risk subgroup had median SUVmax of 14.25 and median ADC of $1.26\text{x}10^{-3}$ mm^2/s and low-risk subgroup had median SUVmax of 14.64 and median ADC of $1.09\text{x}10^{-3}$ mm^2/s. The imaging statistics of high-risk and low-risk subgroups were rather similar (p-value > 0.05). This might indicate that conventional imaging statistics could not reveal differences in survival, while our partitioning approach could.

The volume of the whole tumour is a known biomarker reflecting tumour burden [32–34]. However, surprisingly enough, when we performed survival analysis using whole tumour volume, our result showed the volume of the whole

tumour was not a significant predictor of survival (*p*-value: 0.357). This indicates the entire volume of tumour doesn't always imply the viable tumour component but could include even necrotic or apoptotic portions as well as a non-tumourous component within the tumour. On the other hand, a highly aggressive subregion of the tumour would correlate with the prognosis more strongly and more exclusively, since our patients had stage IV adenocarcinoma. Our study showed that quantitative measure of tumour volume with high aggressiveness was a prognostic factor for survival even if the stage specified by overall tumour burden was the same. Accurate identification of this hot spot, that is, the highly aggressive subregion, would have an additional clinical value by which to judge treatment failure related to the acquired resistance during chemotherapy.

Our study has the following limitations. The sample size was limited because this was a proof-of-concept study, for which we focused on stage IV cancer with an expectation that intratumoural heterogeneity would vary much more in the cases of advanced stage. Among advanced stages, we only included stage IV, histology of adenocarcinoma, patients undergoing platinum-based chemotherapy as a first-line therapy in order to eliminate potential compounding factors affecting prognosis as much as possible. Further studies with larger samples are necessary to validate our findings. There were no pathologic results available to confirm the tumour regions of high aggressiveness, as the recruited patients did not undergo surgery, and therefore histology was unavailable.

In conclusion, we asked if a data-driven clustering approach could identify tumour regions with high aggressiveness within stage IV lung adenocarcinoma tumours using PET and DWI. We also tested whether the identified tumour regions with high aggressiveness predicted survival. Our results showed that identified tumour regions with high aggressiveness were significant predictors of survival.

Funding This study was supported by the Institute for Basic Science (grant number IBS-R015-D1), the National Research Foundation of Korea (grant numbers NRF-2016R1A2B4008545, NRF-2016R1A2B4013046, and NRF-2017M2A2A7A02018568), the Korea Health Technology R&D Project through the Korea Health Industry Development Institute (grant number HI17C0086), and Guerbet Korea Ltd.

Compliance with ethical standards

Guarantor The scientific guarantor of this publication is Ho Yun Lee.

Conflict of interest The authors of this manuscript declare no relationships with any companies, whose products or services may be related to the subject matter of the article.

Statistics and biometry One of the authors has significant statistical expertise.

Informed consent Written informed consent was waived by the Institutional Review Board.

Ethical approval Institutional Review Board approval was obtained.

Methodology
- prospective
- diagnostic or prognostic study
- performed at one institution

References

1. O'Connor JPB, Rose CJ, Waterton JC et al (2015) Imaging intratumor heterogeneity: Role in therapy response, resistance, and clinical outcome. Clin Cancer Res 21:249–257. https://doi.org/10.1158/1078-0432.CCR-14-0990
2. Hanahan D, Weinberg RA (2011) Hallmarks of cancer: The next generation. Cell 144:646–674. https://doi.org/10.1016/j.cell.2011.02.013
3. Shipitsin M, Campbell LL, Argani P et al (2007) Molecular Definition of Breast Tumor Heterogeneity. Cancer Cell 11:259–273. https://doi.org/10.1016/j.ccr.2007.01.013
4. Junttila MR, de Sauvage FJ (2013) Influence of tumour microenvironment heterogeneity on therapeutic response. Nature 501:346–354. https://doi.org/10.1038/nature12626
5. Schmitt MW, Loeb LA, Salk JJ (2016) The influence of subclonal resistance mutations on targeted cancer therapy. Nat Rev Clin Oncol 13:335–347. https://doi.org/10.1038/nrclinonc.2015.175
6. Lee HY, Jeong JY, Lee KS et al (2012) Solitary pulmonary nodular lung adenocarcinoma: correlation of histopathologic scoring and patient survival with imaging biomarkers. Radiology 264:884–893. https://doi.org/10.1148/radiol.12111793
7. Lee G, Lee HY, Park H et al (2017) Radiomics and its emerging role in lung cancer research, imaging biomarkers and clinical management: State of the art. Eur J Radiol 86:297–307. https://doi.org/10.1016/j.ejrad.2016.09.005
8. Ciernik IF, Dizendorf E, Baumert BG et al (2003) Radiation treatment planning with an integrated positron emission and computer tomography (PET/CT): a feasibility study. Int J Radiat Oncol 57:853–863. https://doi.org/10.1016/S0360-3016(03)00346-8
9. Fischer B, Lassen U, Mortensen J et al (2009) Preoperative staging of lung cancer with combined PET-CT. N Engl J Med 361:32–39. https://doi.org/10.1056/NEJMoa0900043
10. Ohri N, Duan F, MacHtay M et al (2015) Pretreatment FDG-PET metrics in stage III non-small cell lung cancer: ACRIN 6668/RTOG 0235. J Natl Cancer Inst 107:1–7. https://doi.org/10.1093/jnci/djv004
11. Lewis DY, Soloviev D, Brindle KM (2015) Imaging tumor metabolism using positron emission tomography. Cancer J 21:129–136. https://doi.org/10.1097/PPO.0000000000000105
12. Gümüştaş S, Inan N, Akansel G et al (2012) Differentiation of malignant and benign lung lesions with diffusion-weighted MR imaging. Radiol Oncol 46:106–113. https://doi.org/10.2478/v10019-012-0021-3
13. Sagiyama K, Watanabe Y, Kamei R et al (2017) Multiparametric voxel-based analyses of standardised uptake values and apparent diffusion coefficients of soft-tissue tumours with a positron emission tomography/magnetic resonance system: Preliminary results. Eur Radiol 27:5024–5033. https://doi.org/10.1007/s00330-017-4912-y
14. Yoon HJ, Kim Y, Kim BS (2015) Intratumoral metabolic heterogeneity predicts invasive components in breast ductal carcinoma in

situ. Eur Radiol 25:3648–3658. https://doi.org/10.1007/s00330-015-3761-9
15. Lee HY, Jeong JY, Lee KS et al (2013) Histopathology of lung adenocarcinoma based on new IASLC/ATS/ERS classification: Prognostic stratification with functional and metabolic imaging biomarkers. J Magn Reson Imaging 38:905–913. https://doi.org/10.1002/jmri.24080
16. Wu J, Cui Y, Sun X et al (2017) Unsupervised clustering of Quantitative image phenotypes reveals breast cancer subtypes with distinct prognoses and Molecular pathways. Clin Cancer Res 23:3334–3342. https://doi.org/10.1158/1078-0432.CCR-16-2415 Personalized
17. Inano R, Oishi N, Kunieda T et al (2016) Visualization of heterogeneity and regional grading of gliomas by multiple features using magnetic resonance-based clustered images. Sci Rep 6:30344. https://doi.org/10.1038/srep30344
18. Metz S, Ganter C, Lorenzen S et al (2015) Multiparametric MR and PET imaging of intratumoral biological heterogeneity in patients with metastatic lung cancer using voxel-by-voxel analysis. PLoS One 10:1–14. https://doi.org/10.1371/journal.pone.0132386
19. Gabow H (2007) Proceedings of the Eighteenth Annual ACM-SIAM Symposium on Discrete Algorithms. Society for Industrial and Applied Mathematics, Philadelphia, PA, USA
20. Levine E, Domany E (2001) Resampling Method for Unsupervised Estimation of Cluster Validity. Neural Comput 13:2573–2593. https://doi.org/10.1162/089976601753196030
21. Paesmans M, Berghmans T, Dusart M et al (2010) Primary tumor standardised uptake value measured on fluorodeoxyglucose positron emission tomography is of prognostic value for survival in non-small cell lung cancer: Update of a systematic review and meta-analysis by the european lung cancer working part. J Thorac Oncol 5:612–619. https://doi.org/10.1097/JTO.0b013e3181d0a4f5
22. Ng S-H, Yen T-C, JT-C C et al (2006) Prospective Study of [18 F]Fluorodeoxyglucose Positron Emission Tomography and Computed Tomography and Magnetic Resonance Imaging in Oral Cavity Squamous Cell Carcinoma With Palpably Negative Neck. J Clin Oncol 24:4371–4376. https://doi.org/10.1200/JCO.2006.05.7349
23. Simon RM, Subramanian J, Li MC, Menezes S (2011) Using cross-validation to evaluate predictive accuracy of survival risk classifiers based on high-dimensional data. Brief Bioinform 12:203–214. https://doi.org/10.1093/bib/bbr001
24. Anderson K, Lutz C, van Delft FW et al (2011) Genetic variegation of clonal architecture and propagating cells in leukaemia. Nature 469:356–361. https://doi.org/10.1038/nature09650
25. Landau DA, Carter SL, Stojanov P et al (2013) Evolution and impact of subclonal mutations in chronic lymphocytic leukemia. Cell 152:714–726. https://doi.org/10.1016/j.cell.2013.01.019
26. Burrell RA, McGranahan N, Bartek J, Swanton C (2013) The causes and consequences of genetic heterogeneity in cancer evolution. Nature 501:338–345. https://doi.org/10.1038/nature12625
27. Horswell S, Matthews N, Swanton C (2013) Cancer heterogeneity and "The struggle for existence": Diagnostic and analytical challenges. Cancer Lett 340:220–226. https://doi.org/10.1016/j.canlet.2012.10.031
28. Schmitz J, Schwab J, Schwenck J et al (2016) Decoding intratumoral heterogeneity of breast cancer by multiparametric in vivo imaging: A translational study. Cancer Res 76:5512–5522. https://doi.org/10.1158/0008-5472.CAN-15-0642 Tumor
29. Divine MR, Katiyar P, Kohlhofer U et al (2016) A Population-Based Gaussian Mixture Model Incorporating 18F-FDG PET and Diffusion-Weighted MRI Quantifies Tumor Tissue Classes. J Nucl Med 57:473–479. https://doi.org/10.2967/jnumed.115.163972
30. Turkki R, Linder N, Holopainen T et al (2015) Assessment of tumour viability in human lung cancer xenografts with texture-based image analysis. J Clin Pathol:1–8. https://doi.org/10.1136/jclinpath-2015-202888
31. Wu J, Gensheimer MF, Dong X et al (2016) Robust Intratumor Partitioning to Identify High-Risk Subregions in Lung Cancer: A Pilot Study. Int J Radiat Oncol Biol Phys 95:1504–1512. https://doi.org/10.1016/j.ijrobp.2016.03.018
32. Kozak MM, Murphy JD, Schipper ML et al (2011) Tumor Volume as a Potential Imaging-Based Risk-Stratification Factor in Trimodality Therapy for Locally Advanced Non-small Cell Lung Cancer. J Thorac Oncol 6:920–926. https://doi.org/10.1097/JTO.0b013e31821517db
33. Henzler T, Goldstraw P, Wenz F et al (2015) Perspectives of Novel Imaging Techniques for Staging, Therapy Response Assessment, and Monitoring of Surveillance in Lung Cancer: Summary of the Dresden 2013 Post WCLC-IASLC State-of-the-Art Imaging Workshop. J Thorac Oncol 10:237–249. https://doi.org/10.1097/JTO.0000000000000412
34. Lee JH, Lee HY, Ahn M-J et al (2016) Volume-based growth tumor kinetics as a prognostic biomarker for patients with EGFR mutant lung adenocarcinoma undergoing EGFR tyrosine kinase inhibitor therapy: a case control study. Cancer Imaging 16:5. https://doi.org/10.1186/s40644-016-0063-7